



Increase in the Frequency of Tropical Deep Convective Clouds with Global Warming¹

Hartmut H. Aumann, Alexander Ruzmaikin and Ali Behrangi
Jet Propulsion Laboratory, California Institute of Technology

Corresponding Author: hhaumann@jpl.nasa.gov

Abstract. Deep Convective Clouds (DCC) are extreme rain events associated with large thunderstorms. They are associated with 0.6% of the area of the tropical oceans. As the tropical oceans warm in a future climate, the frequency of DCC will change. Between 2003 and 2016 the yearly mean temperature of the tropical ocean varied by almost 1K. We use Atmospheric Infrared Sounder (AIRS) data from this time period to derive the probability of the DCC process as function of the Sea Surface Temperature (SST). The onset of the DCC process shifts about +0.5 K per K of warming of the mean tropical ocean SST. When these results are applied to the temperature distribution predicted by CMIP5 climate models for the end of this century, we find that the percent of the area of the tropical oceans associated with DCC, which is 0.6 percent in the current climate, increases to 0.9% , close to a 50% increase.

1. Introduction

The correlation between cloud tops brightness temperatures (bt) detected by infrared sensors from space in the thermal infrared, severe storms and rain rate is well known (e.g., Arkin and Meisner 1987, Vicente et al. 1998 and many more), especially in the tropical zone. We refer to these clouds as Deep Convective Clouds (DCC). The average of the 36 CMIP5 (RCP 8.5) models (Taylor et al. 2012) predicts 2.7 K of warming (range 1.8K to 3.7K) for the oceans between latitudes 30S and 30N, referred to in the following as “tropical ocean”, in the RCP 8.5 scenario by the end of this century. In the following we analyze how much this predict amount of warming will change the frequency of DCC. The DCC frequency is defined as the percent of the area of the tropical oceans (30S to 30N) associated with DCC.

The detection of DCC is instrument and investigator dependent. The simplest method uses an InfraRed (IR) brightness temperature threshold in an 11 μ m atmospheric window channel. Values between 205K and 215K (Gettleman et. al 2002, Liu et al. 2007) are related to the tropopause cold point temperature. We define DCC as any cloud top which satisfies the simple $bt_{900} < 210K$ threshold in a 12 km diameter footprint, where bt_{900} is the brightness temperature of the 11 μ m (900 cm^{-1}) atmospheric window channel in the Atmospheric Infrared Sounder (AIRS, Aumann et al. 2003). Typically AIRS makes 0.7 million observations of the tropical oceans each day, and 4000 of these observations have $bt_{900} < 210K$, i.e. the typical DCC frequency is $4000/700,000 = 0.6\%$. The rain rate reported by AMSR-E (Wilheit, Kummerow and Ferraro 2003), measured about two minutes before the location is identified as DCC by AIRS, is on average 3 mm/hr (Appendix A). These DCC contribute about 17% to the mean rain rate, but are found in only 0.6% of the tropical oceans (30N to 30S). The rapid increase in the observed

¹ © 2017 California Institute of Technology. U. S. Government sponsorship acknowledged



38 frequency of DCC when the SST exceeds 299K, with a peak near 302K, followed by a rapid decrease at higher
39 temperatures, followed by virtually no DCC at SST warmer than 305K was noted decades ago (Gadgil et al., 1984,
40 followed by many papers, e.g. Waliser and Graham 1993). The large seasonal and inter-annual variability of the SST
41 makes it difficult to predict the change in the rain rate in a future climate from the time series derived from the
42 current climate (Gu et al. 2007, Wentz et al 2007). The same problem is encountered with the prediction of the DCC
43 frequency (Aumann and Ruzmaikin, 2013). We largely avoid the problems of time series analysis by deriving the
44 probability of the DCC process as function of the SST from the current climate, and by applying this probability to
45 the distribution of the SST predicted by the climate models.

46

47 2. Data

48

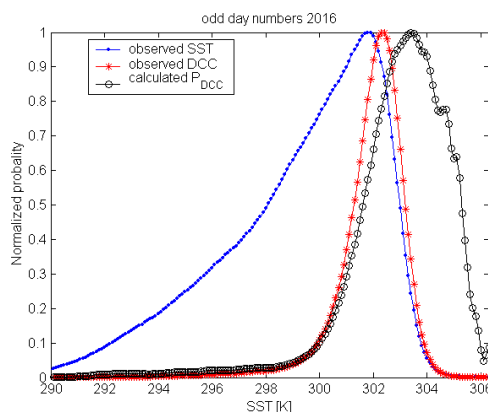
49 2.1. AIRS Data

50 For each DCC identified with AIRS we saved the SST at the DCC location using the NOAA Real Time Global Sea
51 Surface Temperature (RTGSST on a 0.25 degree grid, Thiebaut 2003). These data have been collected every day
52 since 2002. In order to gain insight into DCC process we analyzed the SST associated with each DCC and the
53 average SST between 2003 through 2016. Each year contains on average 2 million DCC. Each year was divided into
54 its even and odd day numbers. This produces 28 groups of data. The DCC in the two groups are observationally
55 uncorrelated. We then determine the distribution of the random sampled SST, and the distribution of the SST
56 associated with a DCC for each of the 28 groups.

57

58 Figure 1 shows the observed distribution of the SST, $N_{SST}(T)$, the observed distribution of the SST associated with
59 DCC, $N_{DCC}(T)$, both normalized to unity, for the odd numbered days from 2016. The distribution functions were
60 evaluated with the Matlab “histc” function with 0.1K wide bins between 280 K and 310 K and a 1K wide
61 rectangular smoothing kernel.

62



63

64

65 Figure 1. The observed probability of SST and DCC and the calculated probability of the DCC process, normalized
66 to one.



67
68 Assume the surface temperature distribution is $PDF_{SST}(T)$, and we have N samples. By definition of a PDF, for N
69 samples of the tropical ocean the number of samples at temperature T , is

$$70 \quad N_{SST}(T) = N * PDF_{SST}(T). \quad (Eq. 1)$$

71
72 The observed count of DCC in these N samples, $N_{DCC}(T)$, is the product of the temperature distribution of the SST
73 with the probability of a temperature dependent DCC process, $P_{DCC}(T)$. $P_{DCC}(T)$ is the probability that a DCC
74 process is associated with a surface temperature T .

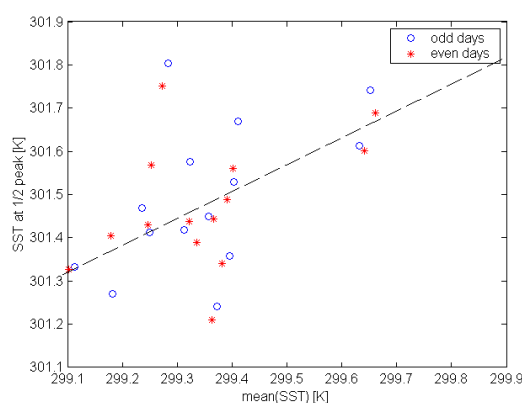
75
76 For $N_{SST}(T)$ samples of the tropical oceans at temperature T

$$77 \quad N_{DCC}(T) = N_{SST}(T) * P_{DCC}(T) \quad (Eq. 2)$$

78
79
80 Then

$$81 \quad P_{DCC}(T) = N_{DCC}(T) / N_{SST}(T), \text{ for all } N_{SST}(T) >> 0. \quad (Eq. 3)$$

82
83
84 The calculated $P_{DCC}(T)$ (normalized to unity) is shown in Figure 1 overlaid on $N_{SST}(T)$ and $N_{DCC}(T)$. $P_{DCC}(T)$ rises
85 steeply for temperatures larger than 300K and reaches a peak near 303K, then drops steeply to zero near 306K. We
86 define the start and end of the DCC process as the temperature where $P_{DCC}(T)$ rises above, then drops below is $1/2$
87 peak value.



88
89
90 Figure 2. The onset of the DCC process as function of mean temperature of the tropical ocean.

91
92 The onset and the end of the DCC formation process was calculated for each of the 28 data groups. The result is
93 shown in Figure 2 as function of the mean tropical SST. Figure 2 shows that the onset of the DCC process increases
94 with the mean temperature of the tropical ocean. The analysis of all 28 data groups results in a slope of $+0.50 \pm 0.18$
95 K/K with warmer SST. This is the convective adjustment of the DCC process. The data from the even and odd days



96 are statistically independent observations of the same DCC process. For the odd days we find a slope of 0.60 K/K,
97 for the even days the slope is 0.41 K/K. The difference of 0.19 K/K is consistent with the 0.18 K/K one sigma
98 uncertainty derived from all data. Within the error bars these results are insensitive to data processing details
99 (Appendix B).

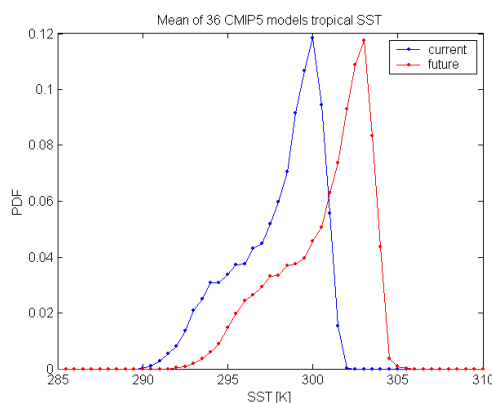
100

101 The end of the DCC process (1/2 peak down probability) is at a temperature of about 304K. We detected no credible
102 temperature sensitivity of the end of the DCC process. In the following calculations we shift the start and end of the
103 DCC process at the same rate. The high temperature cut-off of the DCC process is no sooner than 306K. The data
104 include very few SST or DCC at temperatures warmer than 306K. The 99.9 percentile of all SST and the SST
105 associated with DCC was 306K.

106

107 2.2. Model Data

108 Precipitation and temperature data from 36 state-of-the-art climate model simulations from the fifth Phase of the
109 Coupled Model Intercomparison Project (CMIP5) (Taylor et al., 2012) were used for our analysis of the “current
110 climate” and the “future climate”. Here “current climate” refers to mean historical data from 1976-2005 and “future
111 climate” refers to mean projection from RCP8.5 for the 2070-2100 period. The model output for the tropical ocean
112 SST and rain rate were averaged in 2.5 degree bins of the tropical oceans. Figure 3 shows the Probability Density
113 Function (PDF) of the SST, $PDF_{SST}(T)$ for the current SST (blue) and the future SST (red) using 0.5K wide bins.
114 Except for a shift of about 3K, PDF_{SST} for the current and future temperatures are essentially identical. We conclude
115 that we can approximate the PDF of a warmer ocean by uniformly shifting the PDF_{SST} deduced from the current
116 climate.



117

118

119

120

120 3. Discussion

121

122 3.1. Convective adjustment of the onset of the DCC process.

123

124

There are physical reasons to expect that the threshold for the onset of processes related to deep convection will shift with the temperature and the vertical profiles controlling convective conditional instability (e.g. Williams,

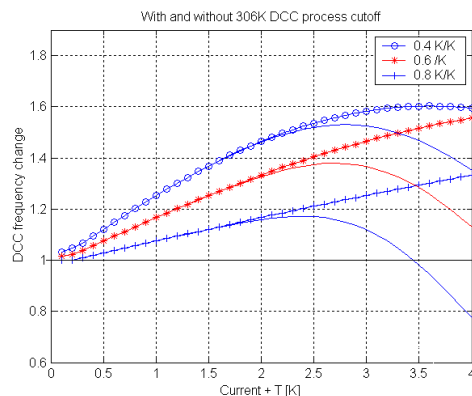


125 Pierrehumbert and Huber 2009, Neelin 2014). The numerical value of this adjustment depends on the process.
126 Johnson and Xie (2010), used a mix of satellite and rain gauge data from between 1980 and 2010 to show significant
127 co-variability between the mean tropical SST and the temperature of the onset of the rain process using a 2 mm/day
128 rain threshold. The same physical reasoning is imbedded in the climate models. Johnson and Xie (2010) reported
129 that the theoretically predicted convective adjustment of the Moist Adiabatic Lapse Rate (MALR), 0.43 K/K, ranges
130 from 0.42 to 0.48 K/K in the CMIP3 models. The temperature of the onset of the rain process for rain rates between
131 2 and 7 mm/day shifts at the rate of 0.98 K/K (range of 0.86 K/K to 1.05K/K) for the 36 CIMP5 models (Appendix
132 C). The DCC process is related to very heavy rain, covering 0.6% of the area of the ocean, while the rain process in
133 the CMIP5 models starts with more moderate rain in a much larger area: The 5 mm/day rain rate covers 23% of the
134 ocean. The observed convective adjustment of the DCC process from our 14 year data record is close to that of the
135 MALR in the CMIP3 models and considerably less than that of the rain process in the CMIP5 models.

136
137

3.2. DCC frequency in a warmer climate

138 For the calculation of the change in the frequency of DCC we used the PDF_{SST} and P_{DCC} calculated from the mean
139 the annual values deduced for the 2003-1016 period. In order to account for the effect of the uncertainty in the
140 convective adjustment we used 0.4 K/K, 0.6 K/K and 0.8 K/K for the DCC convective adjustment, referred as as
141 three scenarios. Figure 4 shows the results from the present to present+4K of warming with 0.1K steps. In the three
142 scenarios the frequency of the DCC increases 27%, 19% and 9% for the first 1K of global warming ($T+1K$), and
143 reaches a peak of 53%, 43% and 23% higher than the present frequency at $T+2.7$ K. In the current climate 0.6% of
144 the area of the tropical oceans is associated with DCC. This increases to between 0.74 to 0.9 percent of the area by
145 the end of the century, close to a 50% increase.



146
147

Figure 4. Change in the DCC frequency with warming ocean.

148

149 It has been argued (e.g. Hartman and Michelson 1993) that at a temperature warmer than about 303K the heat loss
150 due to evaporation starts to exceed the solar incident energy. This decreases the probability of the DCC process.
151 This argument is consistent with the observed peak and subsequent steep roll-off of P_{DCC} seen in Figure 1. Based on
152 our data we know that the high temperature cut-off of the P_{DCC} in the current climate is no sooner than 306K. The
153 thin color-coded lines in Figure 4 show the roll-off of the DCC frequency if we assume a 306K high temperature



154 cut-off of the DCC process. The impact of the 306K cutoff start to become noticeable as a decrease in the DCC
155 frequency no earlier than $T+2.5K$. Our results are not significantly changed by using a 205K or 215K threshold for
156 the definition of DCC.

157

158 As the frequency of DCC increases, the contribution of the DCC rain rate to the total rain rate should increase.
159 However, in order to estimate the magnitude of this effect we need to make a number of uncertain assumptions: 1)
160 Assume that the rain rate associated with DCC in the current climate, 3mm/hr, does not change in a future
161 climate. 2) Assume that the increase in the rain rate is a linear function of the increased number of DCC. 3) Assume
162 that the resulting increase in the rain rate is not compensated for by a decrease in the rain rate for less cold clouds.
163 The need for these assumption makes a quantitative estimate of the change in the total rain rate related to the
164 increase in the DCC frequency uncertain.

165

166 **Summary**

167

168 We derive the probability of the DCC process as function of the Sea Surface Temperature (SST) associated with DCC
169 identified with AIRS between the years 2003 and 2016 for the tropical oceans (30S-30N). During this time the
170 annual mean value of the SST varied by almost 1K, producing measureable shifts in the temperature of the onset of
171 the DCC process. We find that the temperature of the onset of the DCC formation process shifts at the rate of about
172 $+0.50$ K per K of the warming of the mean tropical ocean temperature. We use the probability of the DCC process to
173 predict the change in the frequency of DCC in a future climate, based on the temperature distribution of the tropical
174 oceans predicted by the CMIP5 models. The average of the 36 CMIP5 models (RCP 8.5 scenario) predicts 2.7 K of
175 warming of the mean SST of the tropical oceans by the end of this century. As a result the percent of the area of the
176 tropical oceans associated with DCC, in the current climate 0.6 percent, increases to 0.9% by the end of the century,
177 close to a 50% increase.

178

179 **Acknowledgements**

180

181 The research described in this paper was carried out at the Jet Propulsion Laboratory, California Institute of
182 Technology, under a contract with the National Aeronautics and Space Administration. We are grateful for the
183 unwavering support of Dr. Ramesh Kakar of NASA Headquarters. The daily collection of AIRS DCC, merged with
184 the NOAA SST, is found in the AIRS Calibration Data Subset (ACDS), available freely from the Goddard Earth
185 Sciences Data and Information Services Center <https://disc.gsfc.nasa.gov/AIRS>. The AMSRe data are freely
186 available from ftp://ftp.remss.com/amsre/bmaps_v07/. The CMIP5 RCP 8.5 data can be downloaded from [cmip-
187 pcmdi.llnl.gov/cmip5/data_portal.html](http://pcmdi.llnl.gov/cmip5/data_portal.html)

188

189

190



191 **References.**

192

193 Arkin, P. A., and B. N. Meisner (1987), The relationship between large-scale convective rainfall and cold cloud over
194 the Western-Hemisphere during 1982-84, *Monthly Weather Review*, 115(1), 51-74.

195

196 Aumann, H.H., M.T. Chahine, C. Gautier, M. Goldberg, E. Kalnay, L. McMillin, H. Revercomb, P.W. Rosenkranz,
197 W. L. Smith, D. H. Staelin, L. Strow and J. Susskind, "AIRS/AMSU/HSB on the Aqua Mission: Design, Science
198 Objectives, Data Products and Processing Systems," IEEE Transactions on Geoscience and Remote Sensing,
199 Vol.41.2. pp. 253-264 (2003). The AIRS Calibration Data Subset (ACDS) is a daily product freely available from
200 the GSFC DIS. It includes the spectra of all clouds colder than 225K and their associated SST.

201

202 Aumann H. H. and A. Ruzmaikin, 2013: Frequency of deep convective clouds from ten years of AIRS data, ACP
203 13, 1-39, doi:10.5194/acpd-13-1-2013

204

205 Gadgil, S., P. V. Joseph, and N. V. Joshi, (1984) Ocean-atmosphere coupling over monsoon regions, *Nature*, 312,
206 141-143, 1984.

207

208 Gettelman, A., M.L. Salby and F. Sassi, 2002: Distribution and influence of convection in the tropical tropopause
209 region. *J.Geophys.Res.* 107, D10, doi: 10.1029/2001JD001048.

210

211 Gu, G., Adler, R.F., Huffman, G. J. and Curtis, S. (2007) "Tropical rainfall variability on interannual-to-interdecadal
212 and longer timescales derived from the GPCP monthly product" *J. Clim.* 17, 930-951.

213

214 Hartmann, D. L. and M. L. Michelsen, 1993 Large-scale effects on the regulation of the tropical sea surface
215 temperature, *J. Climate*, 6, 2049-2062.

216

217 Johnson, C. N. and Shang-Ping Xie (2010) "Changes in the sea surface temperature threshold for tropical
218 convection" *Nature.GeoSci.* 7 November 2010, DOI:101038/NCEO1008.

219

220 Liu C., Edward J. Zipser, and Stephen W. Nesbitt (2007) "Global Distribution of Tropical Deep Convection:
221 Different Perspectives from TRMM Infrared and Radar Data (2007) *J. Climate* 20, pp.489-502.

222 Neelin, J. D.,(2014) "Global-warming-changes-and-parameter-sensitivity-deep-convective-statistics-cesm" May 14,
223 2014 in <https://climatemodeling.science.energy.gov/>

224 Thiébaux, J., E. Rogers, W. Wang, and B. Katz (2003), "A new high-resolution blended real-time global sea surface
225 temperature analysis", *Bull. Am. Meteorol. Soc.*, 84(5), 645–656.

226



- 227 Taylor, K. E., R. J. Stouffer, and G. A. Meehl (2012), An overview of CMIP5 and the experiment design, Bull. Am.
228 Meteorol. Soc., 93, 485–498, doi:10.1175/BAMS-D-11-00094.1. Model outputs were collected from the Earth
229 System Grid Federation (ESGF) Peer-to-Peer (P2P) enterprise system, Representative Concentration Pathways
230 (RCP) of 8.5. (<https://pcmdi.llnl.gov/projects/esgf-llnl/>).
231
232 Vicente, G. A., R. A. Scofield, and W. P. Menzel, 1998: The operational GOES infrared rainfall estimation
233 technique. Bulletin of the American Meteorological Society, **79**, 1883-1898.
234
235 Waliser, D.E. and Nicholas E. Graham (1993) Convective Cloud Systems and Warm-Pool Sea Surface
236 Temperatures: Coupled Interactions and Self-Regulation” Journal of Geophysical Research, Vol. 98, No. D7, pages
237 12,881-12,893.
238
239 Wentz, F. J., Ricciardulli, L., Hilburn, K. and Mears, C. (2007) “How much more rain will global warming bring?”
240 Science 317, 233-235.
241
242 Wilheit, T., Kummerow, C.D., and Ferraro, R.: (2003) Rainfall Algorithms for AMSRE, IEEE T. Geosci. Remote,
243 41.2, 204-214.
244
245 Williams, I.N., R. T. Pierrehumbert and M. Huber: (2009) Global warming, convective threshold and false
246 thermostats, GRL. 36. L21805, doi:10.1029/2009GRL039849.
247

248 **Appendix.**

249 250 **A. DCC and Rain rate**

251
252 For the determination of the correlation between DCC and rain rate we used AIRS from every 24th day (135 days)
253 between September 2002 and September 2011. The AMSRe data are used to get the rain rate associated with the
254 positions identified as DCC using the AIRS data. AIRS is +/- 49 degree cross-track scanning with a 1785 km swath
255 width and 15 km average footprint size. AMSRe scans a cone with a 1450 km swath width and we used the 0.25
256 degree gridded product. The area covered by AMSRe is covered about two minutes later by AIRS. AMSRe on EOS
257 Aqua operated from August 2002 through September 2011. The AMSRe data are freely available from
258 ftp://ftp.remss.com/amsre/bmaps_v07/ with an overview in <http://www.remss.com/missions/amsr>.
259

260 The mean rain rate of 0.11 mm/hr was derived from random sampling the AMSRe data in the AIRS swath. The
261 fraction of the mean rain rate associated with a threshold is the fraction of the tropical ocean times the mean rain rate
262 associated with the threshold divided by 0.11. For these data we identified 1,739,919 cloud tops colder than 225K in
263 the tropical oceans. Of these 483,906 satisfied the bt900 <210K condition for DCC. If we define DCC as colder than



264 205K only 255,780 DCC are identified. In Table 1 we summarize average rain rates associated with cold cloud tops
 265 selected with 205K, 210K, 215K and 225K thresholds.

Threshold	205K	210K	215K	225K
Fraction of the tropical oceans associated with the cold cloud	0.0034	0.0064	0.0106	0.0228
Average rain rate [mm/hr]	3.61	3.06	2.61	1.89
False alarm rate	12%	15%	18%	25%
Fraction of total rain	11%	17%	26%	40%
PDF _{DCC} ½ up temperature	301.8	301.6	301.5	301.3

266 Table 1 summarizes results for cold cloud tops selected with 205K, 210K, 215K and 225K thresholds.

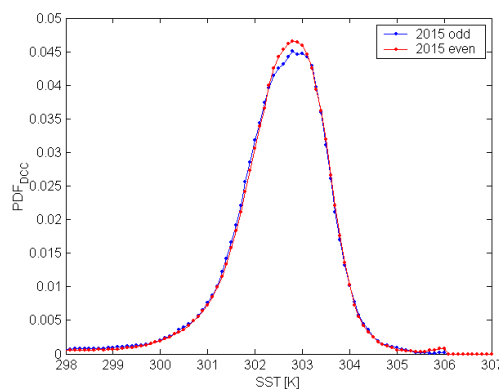
267
 268 The temporal persistence of heavy rain is much shorter than the persistence of associated cold cloud tops. This
 269 temporal mismatch creates the potential for false alarm, i.e. a cold cloud not associated with rain in the AMSRe
 270 record. We define the false alarm fraction as the count of cold clouds with less than 0.1mm/hr of rain divided by the
 271 number of cold clouds associated with each threshold. The false alarm rate for cloud tops warmer than 210K rises
 272 rapidly. The meaning of PDF_{DCC} ½ up will be discussed in Appendix B.

273
 274 The small fraction of the tropical ocean associated with DCC colder than 210K, 0.6% of the area of the tropical
 275 oceans, puts DCC in the class of extreme objects. According to AMSRe, 0.006 of the area of the tropical ocean is
 276 associated with more than 4 mm/hour of rain. Since the average rain rate associated with DCC is only 3 mm/hr, a
 277 considerable fraction of heavy rain is associated with cloud tops not identified as DCC.

278

279 **B. The onset, end and cut-off of the DCC process.**

280



281

282 Figure A1. Determination of the PDF_{DCC} from the even and odd day samples of the same year.

283

284 Figure A1 shows the PDF_{DCC} for a 210K threshold determined from the even and the odd days in 2015. For the
 285 calculation of N_{SST}(T) and N_{DCC}(T) we used the Matlab histc function with a 0.2K wide grid uniformly spaced



286 between 280 and 310K, and the result was smoothed with a 5 point running mean. We define the onset of the DCC
287 process as the temperature where the probability reach $\frac{1}{2}$ of its peak.

288

289 The temperature of the $\frac{1}{2}$ peak of the PDF, the “onset” of the PDF process”, is determined by linear interpolation
290 between the two points closest to the $\frac{1}{2}$ peak point. Figure 2 in the text shows the 28 calculated values of the
291 temperature of the onset of the DCC process and associated tropical ocean mean temperatures for the even and odd
292 day numbers in our data set. The slope, calculated using the Matlab linear least squares fit, is 0.50 K/K with a slope
293 uncertainty of 0.18 K/K. The even and odd days independently sample the same DCC process. For the odd days we
294 find a slope of +0.60 K/K, for the even days the slope is 0.41 K/K. The difference of 0.19 K/K is consistent with the
295 0.18 K/K one sigma uncertainty.

296

297 Alternative numerical methods have been tested on the data, i.e. using the ksdensity function from the Matlab
298 toolbox for the derivation of $N_{SST}(T)$ and $N_{DCC}(T)$. The ksdensity and histc methods produce statistically
299 consistent slope and slope uncertainty estimates. In all numerical experiments the convective adjustment of the DCC
300 process is more than two sigma less than 1K/K.

301

302 We defined the onset of the DCC process as the temperature where the probability reach $\frac{1}{2}$ of its peak with
303 increasing temperature. This is intuitively reasonable. If we use $\frac{1}{3}$ peak for this definition, the temperature of the
304 onset of the DCC process shifts slightly colder for all cases, but the slope of the onset as function of the mean SST is
305 consistent with the slope calculated using the $\frac{1}{2}$ peak.

306

307 The accuracy of the determination of the end of the DCC process is limited by the noise amplification inherent in the
308 deconvolution of $N_{SST,DCC}$ and N_{SST} . Analysis of 14 years of data results in a mean value of 303.7K (range 303.1 to
309 304.5K) with no credible sensitivity to a change in the SST, $+0.57 \pm 0.75$ K/K. Based on our data the cutoff of the
310 DCC process is no sooner than 306 K. The 99.9 percentile of all SST and the SST associated with DCC was 306K.
311 The 99.99 percentile was 307K, but at these high temperatures the RTGSST is seldom validated.

312

313 Is there a high temperature limit to the DCC process? In Figure A1 the probability of the observing a DCC process
314 goes to zero at about 306K. For the 483,906 cold clouds with $t_{900} < 210$ K there are 168 DCC associated with SST
315 warmer than 305K. While there are 5850 SST > 306.1 K in the data covered by the AIRS swath, none are associated
316 with DCC. This suggests that, at least in the current climate, the DCC process stops no sooner than at 306K.

317

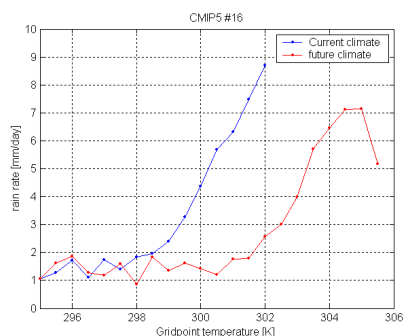
318 **C. Convective adjustment of the rain process in CMIP5 models.**

319

320 The 36 CMIP5 models give the surface temperature and the rain rate in units of mm/day on a 2.5 degree grid for the
321 current climate and the future climate. The blue trace in Figure A2 shows the mean rain rate in 1K wide bins of the
322 surface temperature for the current climate in CMIP5 #16 model. The rain rate increases rapidly as the surface



323 temperature increases above 299K. The red trace shows the rain rate for the future climate in CMIP5#16. The entire
324 pattern is shifted about 3K for the future climate. If we define 5 mm/day as a rain process threshold, the threshold is
325 exceeded at a surface temperature of 300.31K in the current climate, at 303.2K in the future climate. This shift of the
326 temperature of the onset of the rain process to a warmer temperature in a warmer climate is the convective
327 adjustment. A similar pattern is seen in all models for the current and the future climate.



328
329

Figure A2. Dependence of the rain rate on the on the surface temperature

330

331 Between 2 mm/day and 7 mm/day the shift is almost independent of rain rate. The mean convective threshold for the
332 current climate for a 5 mm/day rain rate is 299.6K (range 298.6K to 301.4K). For the future climate the threshold
333 shifts to a mean of 302.3K (range 300.6K to 303.8K). At the same time the mean temperature of the tropical oceans
334 also shifts, depending on the model by between 1.92 K and 3.73K. The ratio of the difference between the
335 convective threshold for the future and current climate and the difference between the future and current mean
336 temperature of the tropical ocean is 0.98 K/K on average, with a range of 0.86 K/K to 1.05K/K. 25% of the area of
337 the current tropical ocean (36 model range 16% to 31%) has a rain rate exceeding 5 mm/day. The roll-off of the
338 rain-rate at temperatures above 305K is shared by all models.